Measurement of Color Invariants

Jan-Mark Geusebroek* Arnold W.M. Smeulders
Rein van den Boomgaard
Intelligent Sensory Information Systems
Faculty of Science, University of Amsterdam
Kruislaan 403, 1098 SJ Amsterdam, The Netherlands
mark@science.uva.nl

accepted by CVPR2000

Abstract

This paper presents the measurement of object reflectance from color images. We exploit the Gaussian scale-space paradigm to define a framework for the robust measurement of object reflectance from color images. Illumination and geometrical invariant properties are derived from a physical reflectance model based on the Kubelka-Munk theory. Imaging conditions are assumed to be white illumination and matte, dull object or general object, respectively, summarized by:

	shadow	highlights	illumination intensity	illumination color
H	+	+	+	–
C	+	–	+	–
W	–	–	+	–
E	–	–	–	–

Invariance is denoted by +, whereas sensitivity to the imaging condition is indicated by –. Invariance, discriminative power and localization accuracy of the color invariants is extensively investigated, showing the invariants to be successful in discounting shadow, illumination intensity, highlights, and noise. Experiments show the different invariants to be highly discriminative while maintaining invariance properties. The presented framework for color measurement is well-founded in physics as well as measurement science. The framework is thoroughly evaluated experimentally. Hence is considered more adequate than existing methods for the measurement of invariant color features.

*This work is sponsored by Janssen Research Foundation, Beerse, Belgium.

1 Introduction

It is well known that color is a powerful cue in the distinction and recognition of objects. Segmentation based on color, rather than just intensity, provides a broader class of discrimination between material boundaries. Color may seem more complex to deal with as it is affected by imaging conditions (illumination color, shadow, geometry). Modeling the physical process of color image formation provides a clue to the object specific parameters [4, 7, 17]. When dealing with color, parameters with known invariance are of prime importance. In this paper we aim at a broad range of diverse color invariant measurement from RGB-cameras.

Differential geometry may be considered as a framework for feature detection and segmentation of images [18, 3]. Embedding the theory in the scale-space paradigm [12, 14] resulted in well-posed differential operators robust against noisy measurements. The Gaussian aperture is the fundamental operator for grey-value scale-space. Introduction of wavelength in the scale-space paradigm, as suggested by Koenderink [13], leads to a spatio-spectral family of Gaussian aperture functions. These color receptive fields are in [6] as the Gaussian color model. As a consequence, the differential geometry framework is extended to the spatio-spectral domain. In the paper we show the geometrically invariant measurement of object color from color images.

In [5], the authors discuss the use of the Shafer model [17], effectively based on the older Kubelka-Munk theory [15], to measure object reflectance independent of illumination color. The Kubelka-Munk theory models the reflected spectrum of a colored body, based on a material dependent scattering and absorption function. The theory has proven to be successful for a wide variety of materials and applications [11, 19]. Therefore, the Kubelka-Munk theory is well suited for determining material properties from color mea-

surements. We derive proper procedures for the measurement of object reflectance, under the assumption of white light and matte, dull object versus general object.

The measurement of invariance involves a balance between constancy of the measurement regardless the disturbing influence on the one hand and retained discriminating power between different objects on the other. As a general rule, for a broader class with a high degree of invariance allowing a larger set of disturbing factors, ignorance of discrimination can be expected. Hence, both invariance and discriminating power of a method should be investigated in balance, yielding complementary information about the methods practical performance. In this paper we extensively investigate invariant properties and discriminative power of the derived color invariants.

The paper is organized as follows. Section 2.1 describes a physical model for image formation, based on the Kubelka-Munk theory. First contribution of this paper is a complete set of invariant expressions derived for basically two different classes of materials (Sect. 2). A second important contribution considers the robust measurement of invariant expressions from RGB-images (Sect. 3). Further, performance of the features as invariance and discriminative power between different colored patches is demonstrated, which may be considered as a third contribution.

2 Determination of Color Invariants

Any method for finding invariant color properties relies on a photometric model and on assumptions about the physical variables involved. For example, hue is known to be insensitive to surface orientation, illumination direction, intensity and highlights, under a white illumination [1, 7]. Normalized rgb is an object property for matte, dull surfaces illuminated by white light. When the illumination color is not white, other object properties should be measured [5]. In this section, expressions for determining invariant properties in color images will be derived for two different classes of objects, matte, dull objects or general objects. When relevant, further specialization as uniform illumination is considered. Note that each essentially different condition of the scene, object and recording circumstances results in different invariant expressions.

2.1 Color Image Formation Model

In [5], image formation is modeled by means of the Kubelka-Munk theory [11, 19] for colorant layers. Under the assumption that light within the material is isotropically scattered, the material layer may be characterized by a wavelength dependent scatter coefficient and absorption coefficient. The model unites both reflectance of light and transparent materials. The class of materials for which the theory is useful ranges from dyed paper and textiles, opaque plastics, paint films, up to enamel and dental silicate cements [11]. The photometric reflectance model resulting from the Kubelka-Munk theory is given by [5]

$$E(\lambda, \vec{x}) = e(\lambda, \vec{x}) \left(1 - \rho_{\mathrm{f}}(\vec{x})\right)^2 R_\infty(\lambda, \vec{x}) + e(\lambda, \vec{x}) \rho_{\mathrm{f}}(\vec{x}) \tag{1}$$

where x denotes the position at the imaging plane and λ the wavelength. Further, $e(\lambda, \vec{x})$ denotes the illumination spectrum and $\rho_{\mathrm{f}}(\vec{x})$ the Fresnel reflectance at $\vec{x}$. The material reflectivity is denoted by $R_\infty(\lambda, \vec{x})$. The reflected spectrum in the viewing direction is given by $E(\lambda, \vec{x})$.

2.2 Invariants for White Illumination

Consider the photometric reflection model (*Eq.* 1). For convenience we first concentrate on the one dimensional case; two dimensional expressions will be derived later. For white illumination, the spectral components of the source are approximately constant over the wavelengths. Hence, a spatial component $i(x)$ denotes intensity variations, resulting in

$$E(\lambda, x) = i(x) \left\{ \rho_{\mathrm{f}}(x) + \left(1 - \rho_{\mathrm{f}}(x)\right)^2 R_\infty(\lambda, x) \right\} \quad . \tag{2}$$

The assumption allows the extraction of expressions describing object reflectance independent of the Fresnel reflectance.

Lemma 1 *Within the Kubelka-Munk model, assuming dichromatic reflection and white illumination, H is an object reflectance property,*

$$H = \frac{\frac{\partial E}{\partial \lambda}}{\frac{\partial^2 E}{\partial \lambda^2}} \tag{3}$$

independent of viewpoint, surface orientation, illumination direction, illumination intensity and Fresnel reflectance coefficient.

Proof: Differentiating (*Eq.* 2) with respect to λ results in

$$\frac{\partial^n E}{\partial \lambda^n} = i(x)(1 - \rho_{\mathrm{f}}(x))^2 \frac{\partial^n R_\infty}{\partial \lambda^n}$$

Hence, ratio of derivatives depend on derivatives of the object reflectance functions R_∞ only, which proves the lemma. □

The property H describes the hue$= \arctan(\lambda_{max})$ of the material. The expression given by Lemma 1 is a fundamental lowest order invariant. Any spatio-spectral derivative of the fundamental invariant is an invariant under the same imaging conditions according to [16].

Proposition 2 *A complete and irreducible set of color invariants, up to a given differential order, is given by all derivatives of the fundamental invariant.*

As a result of Proposition 2, differentiation of the expression for H with respect to x results in object reflectance properties under a white illumination. Note that H is ill-defined when the second order spectral derivative vanishes. We prefer to compute the $\arctan(H)$, for which the spatial derivatives yield better numerical stability.

Corollary 3 *Within the Kubelka-Munk model, a complete and irreducible set of invariants for dichromatic reflection and a white illumination is given by*

$$H_{x^n} = \frac{\partial^n}{\partial x^n}\left\{\arctan\left(\frac{\frac{\partial E}{\partial \lambda}}{\frac{\partial^2 E}{\partial \lambda^2}}\right)\right\} \tag{4}$$

for $n \geq 0$.

Application of the chain rule for differentiation yields the higher order expressions in terms of the spatio-spectral energy distribution. For illustration, we give all expressions up to the first spatial and second spectral order. The derivation of higher order expressions is straightforward. The hue spatial derivative is given by

$$H_x = \frac{E_{\lambda\lambda}E_{\lambda x} - E_\lambda E_{\lambda\lambda x}}{E_\lambda^2 + E_{\lambda\lambda}^2} \tag{5}$$

where $E(\lambda, x)$ is written as E for simplicity, admissible for $E_\lambda^2 + E_{\lambda\lambda}^2 > 0$.

2.3 Invariants for White Illumination and Matte, Dull Surfaces

A tighter class of invariants may be derived when the object is matte and dull. Consider the photometric reflection model (*Eq.* 2), for matte, dull surfaces with low Fresnel reflectance, $\rho_{\mathrm{f}}(\vec{x}) \approx 0$,

$$E(\lambda, x) = i(x) R_\infty(\lambda, x) \ . \tag{6}$$

These assumptions allow the derivation of expressions describing object reflectance independent of the intensity distribution.

Lemma 4 *Within the Kubelka-Munk model, assuming matte, dull surfaces, and a white illumination,* C_λ *is an object reflectance property,*

$$C_\lambda = \frac{1}{E(\lambda, x)}\frac{\partial E}{\partial \lambda} \tag{7}$$

independent of the viewpoint, surface orientation, illumination direction and illumination intensity.

Proof: Differentiation of (*Eq.* 6) with respect to λ and normalization by (*Eq.* 6) results in an object property,

$$\frac{1}{E(\lambda, x)}\frac{\partial E}{\partial \lambda} = \frac{1}{R_\infty(\lambda, x)}\frac{\partial R_\infty}{\partial \lambda}$$

which proves the lemma. □

The property C_λ may be interpreted as describing object color regardless intensity. The normalization by $E(\lambda, x)$ in (*Eq.* 7) is to be evaluated at the spectral wavelength of interest, and therefore is considered locally constant with respect to λ. Again resulting from Proposition 2,

Corollary 5 *Within the Kubelka-Munk model, a complete and irreducible set of invariants for matte, dull surfaces, under a white illumination is given by*

$$C_{\lambda^m x^n} = \frac{\partial^n}{\partial x^n}\left\{\frac{1}{E(\lambda, x)}\frac{\partial^m}{\partial \lambda^m}E\right\} \tag{8}$$

for $m \geq 1, n \geq 0$.

The first order expression is given in (*Eq.* 7). Higher order expressions are given by

$$\begin{aligned} C_{\lambda\lambda} &= \frac{E_{\lambda\lambda}}{E}\ , C_{\lambda x} = \frac{E_{\lambda x}E - E_\lambda E_x}{E^2} \\ C_{\lambda\lambda x} &= \frac{E_{\lambda\lambda x}E - E_{\lambda\lambda}E_x}{E^2}\ . \end{aligned} \tag{9}$$

Note that these expressions are valid everywhere $E(\lambda, x) > 0$. These invariants may be interpreted as the spatial derivative of the intensity normalized spectral slope C_λ and curvature $C_{\lambda\lambda}$.

2.4 Invariants for White and Uniform Illumination and Matte, Dull Surfaces

When it is known that illumination is uniform, consider again the photometric reflection model (*Eq.* 6) for matte, dull surfaces, and a white and uniform illumination with intensity i,

$$E(\lambda, x) = i R_\infty(\lambda, x) \ . \tag{10}$$

The assumption of a white and uniformly illuminated object may be achieved under well defined circumstances, such as the photography of art. These assumptions allow the derivation of expressions describing object reflectance independent of the intensity level.

Lemma 6 *Within the Kubelka-Munk model, assuming matte, dull surfaces, planar objects, and a white and uniform illumination,* W_x *determines changes in object reflectance,*

$$W_x = \frac{1}{E(\lambda, x)}\frac{\partial E}{\partial x} \tag{11}$$

independent of the illumination intensity.

Proof: Differentiation of (*Eq.* 10) with respect to x and normalization by (*Eq.* 10) results in an object reflectance property,

$$\frac{1}{E(\lambda,x)}\frac{\partial E}{\partial x} = \frac{1}{R_\infty(\lambda,x)}\frac{\partial R_\infty}{\partial x} \quad .$$

□

The property W_x may be interpreted as an edge detector specific for changes in spectral distribution. Under common circumstances, a geometry dependent intensity term is present, hence W_x does not represent pure object properties but includes shadow edges when present. The normalization by $E(\lambda, x)$ in (*Eq.* 11) is to be evaluated at the spatial and spectral point of interest, hence is considered locally constant. As a result of Proposition 2,

Corollary 7 *Within the Kubelka-Munk model, a complete and irreducible set of invariants for matte, dull surfaces, planar objects, under a white and uniform illumination is given by*

$$W_{\lambda^m x^n} = \frac{1}{E(\lambda,x)}\frac{\partial^{m+n}}{\partial\lambda^m \partial x^n}E \tag{12}$$

for $m \geq 0$, $n \geq 1$.

Higher order expressions for $E(\lambda, x) > 0$ are given by

$$W_{\lambda x} = \frac{E_{\lambda x}}{E}\,, W_{\lambda\lambda x} = \frac{E_{\lambda\lambda x}}{E} \quad . \tag{13}$$

These invariants may be interpreted as the intensity normalized spatial derivative of the spectral intensity E, spectral slope E_λ and spectral curvature $E_{\lambda\lambda}$.

2.5 Summary of Color Invariants

In conclusion, within the Kubelka-Munk model and assuming white illumination, various invariant sets are derived as summarized in Tab. 1. The class of materials for which the invariants are useful ranges from dyed paper and textiles, opaque plastics, paint films, up to enamel and dental silicate cements [11]. The invariant sets may be ordered by degree of invariance. Combination of invariants open up the way to edge type classification as suggested in [8].

	shadow	highlights	illumination intensity	illumination color
H	+	+	+	–
C	+	–	+	–
W	–	–	+	–
E	–	–	–	–

Table 1. Summary of the various color invariant sets and their invariance to specific imaging conditions. Invariance is denoted by +, whereas sensitivity to the imaging condition is indicated by –. Note that the reflected spectral energy distribution E is sensitive to all the conditions cited.

2.6 Geometrical Color Invariants

So far, we have established color invariant descriptors, based on differential expressions in the spectral and the spatial domain in one spatial dimension. Applied in two dimensions, the result is depending on the orientation of the image content. In order to obtain meaningful image descriptions it is crucial to derive descriptors which are invariant with respect to translation, rotation and scaling. Translation and scale invariance is obtained by examining the (Gaussian) scale-space, which is a natural representation for investigating the scaling behavior of image features [12]. These leads to the same equations as before. For the remaining rotation invariance, Florack *et al.* [3] considers in a systematic manner local gauge coordinates, w and v, aligned to the gradient direction. The first order gradient gauge invariant is the magnitude of the luminance gradient,

$$L_w = \sqrt{L_x^2 + L_y^2} \quad . \tag{14}$$

On the basis of this spatial results, we combine (*Eq.* 14) with the color invariants defined before. Except for the invariant H, two or three measures for edge strength are derived for the different invariants, one for each spectral differential order. Total edge strength due to differences in the energy distribution may be defined by the root squared sum of the edge strengths under a given imaging condition. A summary of total edge strength measures, ordered by degree of invariance, is given in Tab. 2.

3 Measurement of Color Invariants

Up to this point we did establish invariant expressions describing material properties under some general assumptions. These are formal expressions, exploring the infinitely dimensional Hilbert space of spectra at an infinitesimally small spatial neighborhood. The spatio-spectral energy distribution is only measurable at a certain spatial resolution

E	$E_w = \sqrt{E_x^2 + E_{\lambda x}^2 + E_{\lambda\lambda x}^2 + E_y^2 + E_{\lambda y}^2 + E_{\lambda\lambda y}^2}$
W	$W_w = \sqrt{W_x^2 + W_{\lambda x}^2 + W_{\lambda\lambda x}^2 + W_y^2 + W_{\lambda y}^2 + W_{\lambda\lambda y}^2}$
C	$C_w = \sqrt{C_{\lambda x}^2 + C_{\lambda\lambda x}^2 + C_{\lambda y}^2 + C_{\lambda\lambda y}^2}$
H	$H_w = \sqrt{H_x^2 + H_y^2}$

Table 2. Summary of the total edge strength measures for the various color invariant sets, ordered by degree of invariance. The edge strength E_w is not invariant to any change in imaging conditions.

and a certain spectral bandwidth, yielding a limited amount of measurements. Hence, physical realizable measurements inherently imply integration over spectral and spatial dimensions. As suggested by Koenderink [13], general aperture functions, or Gaussians and its derivatives, may be used to probe the spatio-spectral energy distribution.

3.1 The Gaussian Color Model

We follow [6] for the Gaussian color model. Let $E(\lambda)$ be the energy distribution of the incident light, where λ denotes wavelength, and let $G(\lambda_0; \sigma_\lambda)$ be the Gaussian at spectral scale σ_λ positioned at λ_0. Measurement of the spectral energy distribution with a Gaussian aperture yields a weighted integration over the spectrum. The observed energy in the Gaussian color model, at infinitely small spatial resolution, approaches in second order to [13]

$$\hat{E}^{\sigma_\lambda}(\lambda) = \hat{E}^{\lambda_0,\sigma_\lambda} + \frac{\lambda}{\sigma_\lambda}\hat{E}_\lambda^{\lambda_0,\sigma_\lambda} + \frac{1}{2}\frac{\lambda^2}{\sigma_\lambda^2}\hat{E}_{\lambda\lambda}^{\lambda_0,\sigma_\lambda} + \dots \tag{15}$$

where

$$\hat{E}^{\lambda_0,\sigma_\lambda} = \int E(\lambda)G(\lambda;\lambda_0,\sigma_\lambda)d\lambda \tag{16}$$

measures the spectral intensity,

$$\hat{E}_\lambda^{\lambda_0,\sigma_\lambda} = \sigma_\lambda \int E(\lambda)G_\lambda(\lambda;\lambda_0,\sigma_\lambda)d\lambda \tag{17}$$

measures the first order spectral derivative, or yellow-blue, and

$$\hat{E}_{\lambda\lambda}^{\lambda_0,\sigma_\lambda} = \sigma_\lambda^2 \int E(\lambda)G_{\lambda\lambda}(\lambda;\lambda_0,\sigma_\lambda)d\lambda \tag{18}$$

measures the second order spectral derivative, or red-green. Further, G_λ and $G_{\lambda\lambda}$ denote derivatives of the Gaussian with respect to λ. The σ_λ factors are included for scale normalization.

Definition 1 (Gaussian Color Model) *The Gaussian color model measures the coefficients $\hat{E}^{\lambda_0,\sigma_\lambda}$, $\hat{E}_\lambda^{\lambda_0,\sigma_\lambda}$, $\hat{E}_{\lambda\lambda}^{\lambda_0,\sigma_\lambda}$, ... of the Taylor expansion of the Gaussian weighted spectral energy distribution at λ_0 and scale σ_λ.*

Introduction of spatial extent in the Gaussian color model yields a local Taylor expansion at wavelength λ_0 and position $\vec{x_0}$. Each measurement of a spatio-spectral energy distribution has a spatial as well as spectral resolution. The measurement is obtained by probing an energy density volume in a three-dimensional spatio-spectral space, where the size of the probe is determined by the observation scale σ_λ and σ_x. The coefficients of the Taylor expansion of $\hat{E}(\lambda, \vec{x})$ represent the local image structure completely. Truncation of the Taylor expansion results in an approximate representation, optimal in least squares sense. The Gaussian color model approximates the Hering basis [9] for human color vision when taking the parameters $\lambda_0 \simeq 520\,\mathrm{nm}$ and $\sigma_\lambda \simeq 55\,\mathrm{nm}$ [6]. For this case, the measured differential quotients are denoted by $\hat{E}$, $\hat{E}_\lambda$ and $\hat{E}_{\lambda\lambda}$.

It may be concluded from [6] that measurement of spatio-spectral energy implies probing the energy distribution with Gaussian apertures at a given observation scale, resulting in the decomposition of the spatio-spectral energy distribution in its Taylor expansion. Hence, the Gaussian color model describes the differential structure of color images.

3.2 The Gaussian Color Model by a RGB-Camera

In the previous we have defined a general model for measurement of spatio-spectral differential quotients. What remains is a specification of the Gaussian color model for a RGB-camera. It is well known that a RGB-camera approximates the CIE XYZ basis for human color vision by a linear transformation. Further, the first three components $\hat{E}$, $\hat{E}_\lambda$ and $\hat{E}_{\lambda\lambda}$ of the Gaussian color model very well approximate the CIE 1964 XYZ basis when taking $\lambda_0 = 520\,\mathrm{nm}$ and $\sigma_\lambda = 55\,\mathrm{nm}$. Hence, conversion from the measured RGB values to the Gaussian color model is achieved by a linear transformation to fill in next.

A RGB-camera approximates the CIE 1964 XYZ basis for colorimetry by the linear transform [10]

$$\begin{bmatrix}\hat{X}\\ \hat{Y}\\ \hat{Z}\end{bmatrix} = \begin{pmatrix}0.621 & 0.113 & 0.194\\ 0.297 & 0.563 & 0.049\\ -0.009 & 0.027 & 1.105\end{pmatrix}\begin{bmatrix}R\\ G\\ B\end{bmatrix} . \tag{19}$$

The best linear transform from XYZ values to the Gaussian color model is given by [6]

$$\begin{bmatrix}\hat{E}\\ \hat{E}_\lambda\\ \hat{E}_{\lambda\lambda}\end{bmatrix} = \begin{pmatrix}-0.019 & 0.048 & 0.011\\ 0.019 & 0 & -0.016\\ 0.047 & -0.052 & 0\end{pmatrix}\begin{bmatrix}\hat{X}\\ \hat{Y}\\ \hat{Z}\end{bmatrix} . \tag{20}$$

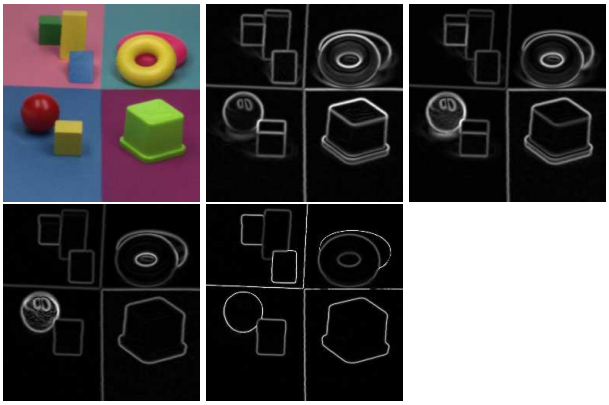

Figure 1. Examples for the total color edge strength measures. Shown are the example image, $\hat{E}_w$, $\hat{W}_w$, $\hat{C}_w$, and $\hat{H}_w$, respectively. Note the effect of intensity edges and highlights having a different response in accordance with Tab. 1 for the various invariants.

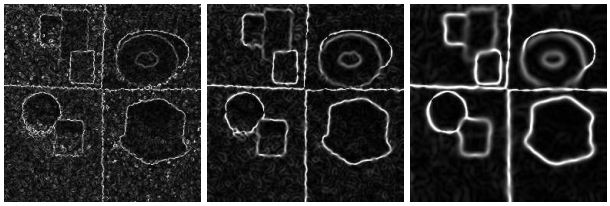

Figure 2. The influence of white additive noise on hue edge detection $\hat{H}_w$. Independent Gaussian zero-mean noise is added to each of the RGB channels, SNR = 5, and edges are determined for $\sigma_x = 1$, $\sigma_x = 2$ and $\sigma_x = 4$ pixels, respectively. Note the noise robustness of the hue gradient $\hat{H}_w$ for larger σ_x.

3.3 Measurement of Geometrical Color Invariants

Measurement of the geometrical color invariants is obtained by substitution of (*Eq.* 20) in the invariant expressions derived in Sect. 2. Measured values for the geometrical color invariants given in Tab. 2 are obtained by substitution of E, E_λ and $E_{\lambda\lambda}$ for the measured values $\hat{E}$, $\hat{E}_\lambda$ and $\hat{E}_{\lambda\lambda}$ at given scale σ_x. The proposed edge strength measures may be ordered by degree of invariance, yielding $\hat{E}_w$ as measure of spectral edge strength, $\hat{W}_w$ as measure of color edge strength, disregarding intensity level, $\hat{C}_w$ as measure of chromatic edge strength, disregarding intensity distribution, and $\hat{H}_w$ as measure of dominant wavelength, disregarding intensity and highlights. An example of the proposed measures is shown in Fig. 1.

Common expressions for hue are known to be noise sensitive. As a consequence of the Gaussian regularization, a trade-off can be made between noise and detail sensitivity. The influence of noise on hue edges H_w for various σ_x is shown in Fig. 2. Gaussian zero-mean noise is added to each color channel, yielding a signal to noise ratio of SNR = 5. The influence of noise on the hue edge detection is drastically reduced for larger observational scale σ_x.

3.4 Discriminative Power for RGB-Recording

In order to investigate the discriminative power of the proposed invariants, edge detection between 1000 different colors of the PANTONE (PANTONE is a trademark of Pantone, inc.) color system is examined. Therefore, uncoated patches from a printed color book (PANTONE color formula guide 1000 printers edition 1992-1993, Groupe BASF, Paris, France) containing 1013 PANTONE colors are recorded by a RGB-camera (Sony DXC-930P), under a 5200K daylight simulator (Little Light, Grigull, Jungingen, Germany). Purely achromatic patches are removed from the set, leaving 1000 colored patches. In this way, numerically unstable result for set $\hat{H}$ are avoided.

Color edges are formed by combining each of the patches with all others, yielding 499,500 different edges. The total edge strength measures for invariants $\hat{E}$, $\hat{W}$, $\hat{C}$, and $\hat{H}$ (Tab. 2) are measured for each color combination at a scale of $\sigma_x = \{1, 2, 4\}$ pixels, hence evaluating the total performance of each set of invariants. Discrimination between colors is determined by evaluating the ratio of discriminatory contrast between patches to within patch noise,

$$DNR_c(i,j) = \frac{\hat{c}_{ij}}{\max_k \sqrt{\frac{1}{N^2}\sum_{x,y} \hat{c}_k(x,y)^2}} \qquad (21)$$

where c denotes one of the edge strength measures for $\hat{E}$, $\hat{W}$, $\hat{C}$, or $\hat{H}$, respectively. Further, $\hat{c}_{ij}$ denotes the edge strength between patch i and j, and $\hat{c}_k$ denotes the responses of the edge detector to noise within patch k. Hence, for detector c, the denominator in expression (*Eq.* 21) expresses the maximum response over the 1000 patches due to noise, whereas the numerator expresses the response due to the color edge. Two colors are defined to be discriminable when $DNR \geq 5$, effectuating a very conservative threshold.

The results of the experiment are shown in Tab. 3. For colors uniformly distributed in color space, and for the configuration used and spatial scale $\sigma_x = 1$, about 950 colors can be distinguished from one another ($\hat{E}$). Lowest discriminative power is achieved by invariant set $\hat{H}$, which discriminates approximately 300 colors. For invariant $\hat{C}$, performance increases to 600 colors. A further increase is for $\hat{W}$, which distinct between 900 colors. When the spa-

	$\sigma_x = 1$	$\sigma_x = 2$	$\sigma_x = 4$
$\hat{E}$	930	990	1000
$\hat{W}$	903	997	999
$\hat{C}$	598	860	917
$\hat{H}$	308	316	376

Table 3. For each invariant, the number of colors is given which can be discriminated from one another in the PANTONE color system (1000 colors). The number refers to the amount of colors still to be distinguished with $DNR > 5$ given the hardware and spatial scale σ_x. For $\sigma_x = 2$ and $\sigma_x = 4$, $\hat{E}$ and $\hat{W}$ discriminate between all patches, hence the results are saturated.

tial scale σ_x increases, discrimination improves. A larger spatial scale yields better reduction of noise, hence a more accurate estimate of the true color is obtained. The results shown for $\sigma_x = 2$ and $\sigma_x = 4$ are saturated for $\hat{E}$ and $\hat{W}$. Hence, a larger set of colors can be discriminated than shown here. Note that the power of discrimination expressed as the amount of discriminable colors is inversely proportional to the degree of invariance. These are very encouraging results given a standard RGB-camera and not a spectrophotometer. To discriminate 300 to 950 colors while maintaining invariance on just two patches in the image is helpful for many practical image retrieval problems.

3.5 Scene Geometry Invariance

In this section, illumination and viewing direction invariance is evaluated by experiments on a collection of real-world surfaces. Colored patches from the CUReT (http://www.cs.columbia.edu/CAVE/curet/) database are selected [2], disregarding patches for which saturation is of major influence. Hence, recordings of 25 material patches, each captured under 205 different illumination and viewing directions are considered. The total edge strength measures for invariants $\hat{E}$, $\hat{W}$, $\hat{C}$, and $\hat{H}$ (Tab. 2) are obtained for each imaging condition, yielding a total of 20,910 different edge strengths for one material. The root squared sum over the measured edge strengths indicates sensitivity to the scene geometry for the material and edge strength measure under consideration. For the spectral edge strength E, edge strength is normalized to the average intensity over all materials and all viewing conditions. In this way, comparison between the various edge strengths is possible. The results are shown in Tab. 4. A high value of $\hat{E}$ indicates influence of scene geometry on material surface reflectance. A low value for the invariants $\hat{H}$, $\hat{C}$, or $\hat{W}$, relative to $\hat{E}$, indicate robustness against illumination direction, viewing direction, and object geometry. The invariant W is shown to

material	$\hat{H}$	$\hat{C}$	$\hat{W}$	$\hat{E}$
Pebbles	16.0	5.1	14.7	14.5
Artificial Grass	2.5	3.2	37.0	54.9
Cork	15.9	26.0	34.9	76.3
Rug	17.4	8.6	42.8	72.9
Sponge	15.0	13.5	30.0	70.5
Lambswool	15.1	7.2	29.2	86.5
Lettuce Leaf	30.2	15.3	62.0	44.6
Rabbit Fur	11.8	4.7	24.4	55.6
Quarry Tile	28.9	48.1	51.2	100.7
Human Skin	14.1	3.7	31.3	81.2
Straw	10.6	3.0	34.7	64.9
Brick	29.2	63.9	64.1	95.5
Corduroy	15.6	2.5	22.0	56.2
Linen	20.1	3.1	30.0	67.2
Brown Bread	12.9	14.9	32.6	41.8
Corn Husk	6.3	2.3	19.8	50.2
Soleirolia Plant	1.7	5.5	27.8	31.1
Wood a	11.0	4.2	36.6	82.5
Orange Peel	21.9	17.1	33.2	81.1
Wood b	10.2	4.7	25.0	36.8
Peacock Feather	23.6	5.9	48.7	60.1
Tree Bark	15.2	5.4	22.5	15.2
Cracker a	6.9	2.7	19.3	14.8
Cracker b	8.5	4.8	27.1	24.1
Moss	4.7	4.7	54.2	75.0

Table 4. Results for scene geometry invariance evaluation. A low value for the variation of invariants $\hat{H}$, $\hat{C}$, or $\hat{W}$ relative to $\hat{E}$ indicate robustness against scene geometry. Note that $\hat{W}$ is highly sensitive to scene geometry, $\hat{C}$ reduces variation drastically, whereas $\hat{H}$ remains approximately constant for highly specular materials.

be highly sensitive to scene geometry, as expected. For non-planar patches, $\hat{W}$ is influenced by shading effects, causing variance $\hat{W} > \hat{E}$. Highly specular materials show low variance in $\hat{H}$. Overall, variance for $\hat{H}$ is higher than for $\hat{C}$, which is due to amplification of variation in observed color. Even for these non-Lambertian surfaces, invariant set $\hat{C}$ is highly robust against changes in scene geometry. These results demonstrate the usefulness of the various invariant sets for material classification and recognition, based on surface reflectance properties.

4 Conclusion

In this paper, we have derived geometrical color invariant expressions describing material properties for two classes of materials, matte, dull object or general object, assuming a white illumination. The reflectance model under which the invariants remain valid is useful for a wide range of materials [11]. Furthermore, we have established the robust measurement of object reflectance from RGB-images, based on the Gaussian scale-space paradigm. Experiments on an example image showed the invariant set C to be successful in disregarding shadow edges, whereas the set H is shown to

be successful in discounting both shadow edges and highlights. In [5], the authors have investigated invariant properties assuming a colored illumination.

We showed the discriminative power to be orderable by degree of invariance. Highest discriminative power is obtained by set W which has the smallest set of disturbing conditions, namely overall illumination intensity or camera gain. Discrimination degraded for set C, which is invariant for shading effects, whereas invariant set H, invariant for shadows and highlight, has lowest discriminative power. Discriminating power is increased when considering a larger spatial scale σ_x, resulting in a more accurate estimate of color value. The aim of the paper is reached in that high color discrimination resolution is achieved while maintaining constancy against disturbing imaging conditions, both theoretically as well as experimentally.

We have restricted ourselves in several ways. First, we have derived expressions up to the second spatial order, and investigated their performance only for the spatial gradient. The derivation of higher order derivatives is straightforward. Secondly, we have only considered spectral derivatives up to second order, yielding compatibility with human color vision. For a spectrophotometer, measurements can be obtained at different positions λ_0, for different scales σ_λ, and for higher spectral differential order, thereby exploiting the generality of the Gaussian color model. Finally, we have not shown the evolution of features in color scale-space. The Gaussian color model is the natural operator to achieve scale independency in color feature detection.

We have demonstrated the Gaussian color model to be highly robust for perturbations in the color image. The Gaussian color model extents the differential geometry approaches from grey-value images to multi-spectral differential geometry. The presented framework for color measurement is well-defined on a physical basis, hence it is theoretically better founded as well as experimentally better evaluated than existing methods for the measurement of color features in RGB-images.

References

[1] R. Bajcsy, S. W. Lee, and A. Leonardis. Color image segmentation with detection of highlights and local illumination induced by inter-reflections. In *IEEE 10th International Conference Pattern Recognition '90*, pages 785–790, Atlantic City, New Jersey, 1990.

[2] K. J. Dana, B. van Ginneken, S. K. Nayar, and J. J. Koenderink. Reflectance and texture of real world surfaces. *ACM Trans Graphics*, 18:1–34, 1999.

[3] L. M. J. Florack, B. M. t. H. Romeny, J. J. Koenderink, and M. A. Viergever. Cartesian differential invariants in scale-space. *Journal of Mathematical Imaging and Vision*, 3(4):327–348, 1993.

[4] R. Gershon, D. Jepson, and J. K. Tsotsos. Ambient illumination and the determination of material changes. *J. Opt. Soc. Am. A*, 3:1700–1707, 1986.

[5] J. M. Geusebroek, A. Dev, R. van den Boomgaard, A. W. M. Smeulders, F. Cornelissen, and H. Geerts. Color invariant edge detection. In *Scale-Space Theories in Computer Vision*, pages 459–464. Springer-Verlag, 1999.

[6] J. M. Geusebroek, R. van den Boomgaard, A. W. M. Smeulders, and A. Dev. Color and scale: The spatial structure of color images. In *submitted to the Sixth Europian Conference on Computer Vision (ECCV)*, 26th June-1st July, 2000.

[7] T. Gevers and A. W. M. Smeulders. Color based object recognition. *Pat. Rec.*, 32:453–464, 1999.

[8] T. Gevers and H. Stokman. Reflectance based edge classification. In *Proceedings of Vision Interface*, pages 25–32. Canadian Image Processing and Pattern Recognition Society, 1999.

[9] E. Hering. *Outlines of a Theory of the Light Sense*. Harvard University Press, Cambridge, MS, 1964.

[10] ITU-R Recommendation BT.709. Basic parameter values for the HDTV standard for the studio and for international programme exchange. Technical Report BT.709 [formerly CCIR Rec. 709], ITU, 1211 Geneva 20, Switzerland, 1990.

[11] D. B. Judd and G. Wyszecki. *Color in Business, Science, and Industry*. Wiley, New York, NY, 1975.

[12] J. J. Koenderink. The structure of images. *Biol. Cybern.*, 50:363–370, 1984.

[13] J. J. Koenderink and A. Kappers. *Color Space*. Utrecht University, The Netherlands, 1998.

[14] J. J. Koenderink and A. J. van Doorn. Receptive field families. *Biol. Cybern.*, 63:291–297, 1990.

[15] P. Kubelka. New contribution to the optics of intensely light-scattering materials. part i. *J. Opt. Soc. Am.*, 38(5):448–457, 1948.

[16] P. Olver, G. Sapiro, and A. Tannenbaum. Differential invariant signatures and flows in computer vision: A symmetry group approach. In B. M. ter Haar Romeny, editor, *Geometry-Driven Diffusion in Computer Vision*. Kluwer Academic Publishers, Boston, 1994.

[17] S. A. Shafer. Using color to separate reflection components. *Color Res. Appl.*, 10(4):210–218, 1985.

[18] B. M. ter Haar Romeny, editor. *Geometry-Driven Diffusion in Computer Vision*. Kluwer Academic Publishers, Boston, 1994.

[19] G. Wyszecki and W. S. Stiles. *Color Science: Concepts and Methods, Quantitative Data and Formulae*. Wiley, New York, NY, 1982.